# Structural Preablation Dynamics of Graphite Observed by Ultrafast Electron Crystallography

Fabrizio Carbone,[1] Peter Baum,[1] Petra Rudolf,[2] and Ahmed H. Zewail[1]

[1]*Physical Biology Center for Ultrafast Science & Technology, Arthur Amos Noyes Laboratory of Chemical Physics, California Institute of Technology, Pasadena California, 91125, USA*

[2]*Zernike Institute for Advanced Materials, University of Groningen, Nijenborgh 4, NL-9747AG Groningen, The Netherlands*

(Received 15 October 2007; published 22 January 2008)

By means of time-resolved electron crystallography, we report direct observation of the structural dynamics of graphite, providing new insights into the processes involving coherent lattice motions and ultrafast graphene ablation. When graphite is excited by an ultrashort laser pulse, the excited carriers reach their equilibrium in less then one picosecond by transferring heat to a subset of strongly coupled optical phonons. The time-resolved diffraction data show that on such a time scale the crystal undergoes a contraction whose velocity depends on the excitation fluence. The contraction is followed by a large expansion which, at sufficiently high fluence, leads to the ablation of entire graphene layers, as recently predicted theoretically.

DOI: 10.1103/PhysRevLett.100.035501 PACS numbers: 61.82.−d, 07.78.+s, 63.20.K−, 78.47.−p

The unique semimetal physical properties of graphite and its chemical inertness make possible numerous applications [1–3] including the use in nuclear reactors [4,5]. When subjected to a shock, the structure distorts, and the ablation to form graphene [6] may result from its instability. It is of fundamental importance to visualize the associated dynamics with atomic-scale spatial and temporal resolutions. Here, by means of ultrafast electron crystallography, we report direct observation of the structural dynamics of graphite following an impulsive near infrared excitation. The diffraction shows that the structure of graphite first contracts perpendicular to the layer planes on the time scale of 0.5 to 3 ps, depending on fluence, and then nonthermally expands in 7 ps. The excitation fluence dependence of both processes indicates a distinct behavior. The highly anisotropic transfer of carrier energy to a subset of phonons of the quasi-2D-structure alters the forces between layers which control the time scale and amplitude of structural change. These atomic motions on different time scales for compression, expansion and restructuring determine the degree of the instability, which at sufficiently high fluences reaches that of graphene ablation [7,8], as predicted theoretically [9].

Previous optical studies have focused on the carrier dynamics induced by both high [10,11] and low fluence [12] optical excitation, revealing features of the unique phonon excitations in quasi-two-dimensional graphite and the coherent modes involved. In order to resolve details of the structure, diffraction is our method of choice. In ultrafast electron crystallography, the probing wavelength is 0.07 Å at 30 keV electron acceleration energy, and we use femtosecond (fs) near infrared pulses (800 nm) for the optical excitation of the $\pi$ system of graphite. The overall resolution is determined by group velocity mismatch [13], but as shown here, by tilting the optical wave front, see the inset in Fig. 4, we are able to resolve subpicosecond coherent dynamics. Highly oriented and single crystal graphite were studied, and indeed the static diffraction patterns of both display the characteristic structural features of the material. Typical electron diffraction patterns are displayed in Fig. 1. The narrow and intense Bragg spots confirm the good quality of the crystal investigated. From these patterns we obtained the lattice dimensions of $a = b = 2.46$ Å, and $c = 6.7$ Å, which are in agreement with the reported values obtained from static neutron diffraction [14]. In order to enhance the contribution of interferences of bulk layers, we tuned the angle of incidence of the electrons so that the beam specular reflection coincides with the (0 0 14) Bragg spot, whose profile is displayed as an inset in Fig. 3. However, we have also studied in detail other diffraction spots such as (0 0 6), and (0 0 8).

The experiments were carried out on a natural single crystal of graphite and, for comparison, on a highly ori-

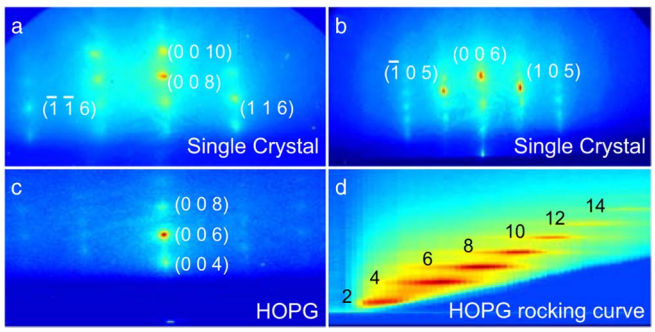


FIG. 1 (color online). Graphite diffraction patterns. (a) and (b) Static electron diffraction from a single crystal along two different zone axes. The lattice constants are $a = 2.46$ Å and $c = 6.7$ Å and all Bragg spots can be identified. (c) Diffraction pattern of a highly ordered graphite crystal also showing the direct attenuated nondiffracted spot (lower edge). (d) Rocking curve ($\theta$ dependence, in the range $\theta = 0$ to 4°) for measuring the $c$-axis value of a highly ordered graphite crystal. For this material $c$ is also 6.7 Å.

 

ented pyrolytic graphite (HOPG) commercially available from Goodfellow. Both samples, HOPG and single crystals, have similar dynamics; because the single crystal displays sharper diffraction spots and better order, we will focus on the data obtained from the latter. The single crystal came from Siberia; high quality angle resolved photoemission spectroscopy data were obtained from the crystal, revealing the features of bulk graphite's electronic structure [15]. The surfaces of both samples were cleaved immediately before introducing into the vacuum chamber which maintains a pressure of $8 \times 10^{-10}$ Torr. The sample was excited by laser pulses of 120 fs duration at a wavelength $\lambda = 800$ nm. The electron pulses were spatially overlapped on the surface and probed the reaction of the lattice to the pump, whose fluence was varied in the range between 3.5 mJ/cm$^2$ and 44.5 mJ/cm$^2$.

Following laser excitation, Bragg spots of the diffraction pattern show unique changes in position, intensity and width, corresponding to changes in the crystal structure of the investigated material. In panel (a) of Fig. 2 we present the measured position of the (0 0 14) Bragg spot as a function of the time delay between the fs excitation and electron pulses, and at different excitation fluences. These transients were obtained in steps of 250 fs and span a time scale of 10 ps; below, the behavior at longer times will be shown. The position of a Bragg spot directly images the expansion or compression of the lattice in the probed direction. Thus the results shown for the observed shift of the (0 0 14) Bragg spot indicate an initial compression which is followed by an expansion along the $c$ axis. The evolution of the corresponding intensity is displayed in panel (c) of Fig. 2. In a previous study of gold nanoparticles [16] on graphite, a contraction of the substrate was mentioned and used as an indicator of the temporal resolution of the apparatus.

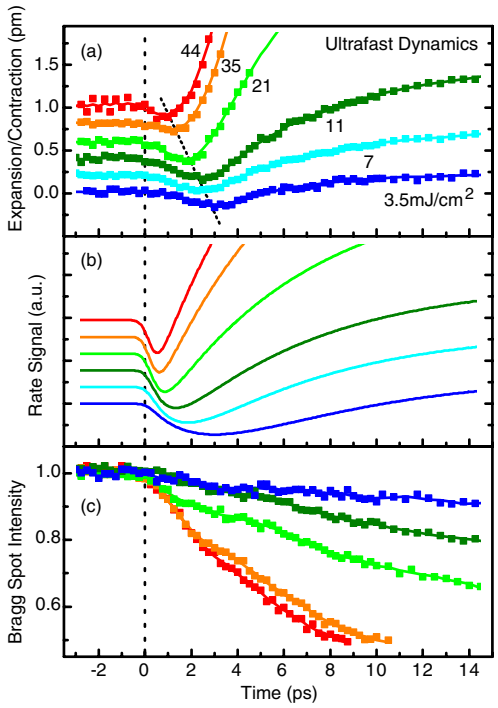


FIG. 2 (color online). Ultrafast dynamics. (a) time dependence of lattice compression or expansion for different excitation fluences. The curves are vertically shifted for better visibility, and the given scale is for the 3.5 mJ/cm$^2$ case. (b) The results of a kinetic model (see text) involving two processes, that of expansion driven by the fraction of energy delivered to the lattice, and the second is a fluence dependent rate constant describing the early time compression. The characteristic time of the compression is found to range between 0.2 ps and 2.5 ps at the lowest and highest fluence, respectively. The time constant for expansion is 7 ps at all fluences but the amplitude increases as fluence increases. (c) Time dependence of the (0 0 14) Bragg-spot intensity. This spot becomes the most intense when $\theta$ is optimized (see inset of Fig. 3).

The compression and expansion processes show different dependencies on excitation fluence. The maximum of the compression occurs with progressive delay as the fluence deposited into the crystal is decreased, as indicated by the guide to the eye line in panel (a) of Fig. 2. The time constant of the expansion is not affected by the laser fluence, and a common inflection point is noted at 3 to 4 ps, which marks a transition for the dynamics of processes involved: one occurring at early times and another at longer time which results in the expansion. To account for an overall change of rates and the fluence dependence, we invoked a simple model describing population flow as a sum of two-rate processes for the compression and expansion [Fig. 2 panel (b)]. It is found from the solution that the expansion has a constant rate of 7 ps for all excitation fluences, consistent with a direct fitting of an exponential rise to the transient at long time.

The expansion amplitude scales linearly with the fluence, showing that the excited carriers directly contribute to the nonthermal expansion observed in 7 ps. For the compression, however, the change of the rate with fluence accounts for the observed trend in Fig. 2. As discussed below, the initial step involves the anisotropic carriers excitation and select phonon dynamics, while the expansion is the result of a nonequilibrium lattice "temperature." It should be noted that what was expected to observe is the expansion and its increased amplitude with fluence [17], but in addition here we observe the contraction which is significant in describing structural instabilities and ablation of graphite. Finally, the changes in the Bragg-spot intensity, panel (c) of Fig. 2, are consistent with the behavior of the shift, an initial intensity decay on a similar time scale followed by a slower decay, with increased intensity depletion as fluence increases. The width (not shown here) increases with time, showing the expected dynamical inhomogeneity of the lattice.

In order to gain more insight into the nature of the expansion, we obtained the derivative [18] of the Bragg peak position as a function of time. The results are displayed in the top panel of Fig. 3, over the first 10 ps. The maximum in the derivative indicates a change in the rate of

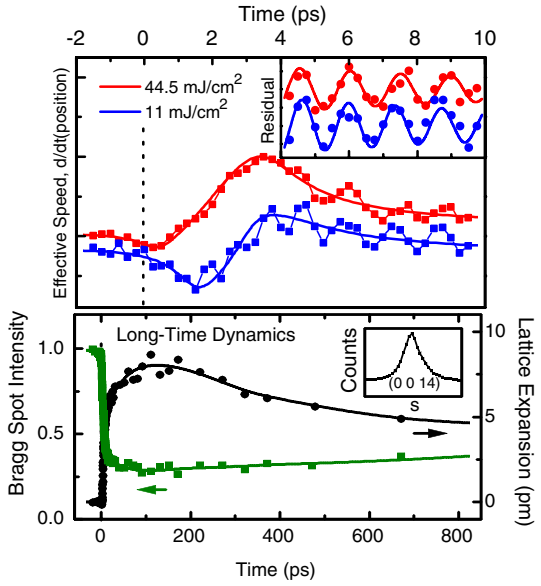


FIG. 3 (color online). Top panel: Coherent lattice oscillations. The derivative as a function of time of the (0 0 14) Bragg-spot position is displayed for the 44 mJ/cm$^2$ (red) and 11 mJ/cm$^2$ (blue) excitation fluences. The blue trace is magnified by a factor of 6 for display. The inset shows the residual of an exponential fit to the data between 4 and 10 ps (see text). Bottom panel: Restructuring observed in position and intensity changes of diffraction. The position and intensity of the (0 0 14) Bragg spot, whose profile is displayed in the inset, are shown for a fluence of 44.5 mJ/cm$^2$.

the Bragg peak shift (inflection point). However, its position is relatively insensitive to the fluence, contrary to the contraction behavior, suggesting that following expansion the strongly coupled optical phonons have a characteristic time scale ($\simeq$5–7 ps) for transferring the energy into other modes by anharmonic couplings [18,19]. The most striking feature in Fig. 3 is the observation of a coherent oscillation with a period of about 1 ps, best visible in the range between 4 and 10 ps. The inset of Fig. 3 shows the residual after subtraction of an exponential decay for two different laser fluences, and the period is obtained by a sinusoidal fit. This oscillation is reproducible for different positions on the sample. The long-time restructuring is evident in the diffraction pattern, as shown in the bottom panel of Fig. 3, at a fluence of 44.5 mJ/cm$^2$. The graph displays the vertical position changes of the (0 0 14) Bragg spot, and at the same time its intensity change, now over the range of 800 ps. The Bragg peak intensity mirrors the expansion or restructuring with a decrease first, due to the position disorder of the atoms within the unit cell, and then a recovery toward the original structure on the nanosecond time scale.

From these results of the ultrafast, and up to ns, structural dynamics, the following picture is provided. With impulsive laser excitation the electronic bands are populated anisotropically, and, because energy and momentum have to be conserved, these carriers can excite only large momentum phonons. Such selective coupling leads to an efficient excitation of a subset of vibrations [20,21], so-called strongly-coupled-optical-phonons (SCOP), which ultimately decay to yield other vibrations. Because of electron-electron scattering the initial fs carrier excitation acquires a broadening in the energy distribution [10,20], and this distribution relaxes by electron-phonon coupling, leading to SCOP in the case of graphite. The time scale has been estimated to be on the order of 500 fs, for the electron-phonon-coupling process, and 5 to 7 ps for the decay of SCOP into other modes [20,21]. These two characteristic time constants were obtained from time-resolved photoemission and THz spectroscopy experiments [20,21]. Experimental and theoretical studies have both indicated that the mechanism for selective excitation of a subset of phonon modes in graphite is due to its anisotropic band structure combined with a particularly strong electron-phonon coupling [20–24]. At 1.5 eV, the laser pulses effectively excite electrons in the vicinity of the $M$ point of the band dispersion, which corresponds to a van Hove singularity in the density of states [21], and because of symmetry SCOP are produced with high efficiency.

The initial compression of the interplanar distance, which occurs with a characteristic time as fast as 500 fs depending on the laser fluence, suggests that such phenomenon is mediated by the cooperative motion induced by the phonon subset, prior to their decay in 5–7 ps, and the out of equilibrium electronic structure driven by the potential of the excited carriers. Because of the band anisotropy of the electronic structure, the electrons excited from the $\pi$ to the $\pi^*$ band preferentially weaken the $c$-axis bond, and cause the observed $c$-axis dynamics, similar to what is observed in germanium using Raman spectroscopy and pump-probe reflectivity measurements [18,19]. Thus, it is reasonable to expect that in the quasi-2D-structure, depending on the carrier density (fluence) in the layers, the force changes between them and hence the rate. Considering the recent theoretical study of ablation at high fluences our results represent the preablation regime. In fact when extrapolating the expansion time exponentially to the high fluence theoretical results (170 mJ/cm$^2$) [9], we obtained the predicted time scale, but within a factor of 3, for ablation and graphene expulsion.

The observed coherent oscillation during $c$-axis expansion clearly indicates the direct role of SCOP in the initial dynamics. The period of $\simeq$1 ps reported here is consistent with the $c$-axis optical phonon frequencies (obtained from inelastic neutron scattering [25]), which cover the range of $\nu_{\mathrm{op}}^{-1} \simeq 0.7$–$1.4$ ps. The observed oscillation in the time-resolved spectra [12] was assigned to a vibration ($E_{2g}$) shear mode (43 cm$^{-1}$), which gives a period of $\simeq 0.8$ ps. The overall expansion of the lattice, which can be as much as 0.08 Å at the highest fluence of 44.5 mJ/cm$^2$, corresponds to 1.25% of the $c$-axis equilibrium value, 6.7 Å. This expansion is huge and beyond any thermal value. The thermal linear expansion coefficient ($\alpha = \frac{\Delta L}{L_0}\frac{1}{\Delta T}$, with $L$

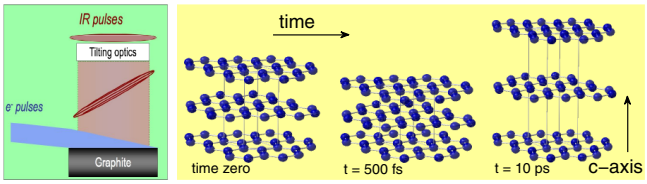


FIG. 4 (color online). The graphite crystal structure at different times. The schematic displays the movements of planes, exaggerated for clarity. The time scales in this graph correspond to the observation at a laser fluence of 44 $mJ/cm^2$. The time scales at different fluences can be seen in Fig. 2. On the left, a schematic is shown for the optical tilting arrangement used here to reach the fs resolution in reflection (see text).

being the expansion and $\Delta T$ the temperature change) for graphite is $7.9 \times 10^{-6}$ $K^{-1}$ [6], and such change would correspond to a temperature jump of more than 1500 K. Given our fluence and the heat capacity of graphite, the maximum expected temperature rise is around 40 K.

Finally, the reported experimental results suggest further theoretical examination with MD simulations. The time-dependent *ab initio* calculations, reported in Ref. [9], predict that ablation of graphene layers under laser irradiation results as a consequence of the strong repulsion between different planes, following an initial significant decrease of their relative distance. This ablation may occur at a fluence below the damage threshold, which corresponds to the fluence necessary to break the in-plane bonds. At the high fluence, the initial collision between planes is estimated to be on tens of femtoseconds, while ablation of layers is on the picosecond time scale. Our results support this collision model which requires major preablation structural instability. However, in the theoretical simulations it was assumed that excited carriers reach their equilibrium with the lattice in 10 fs. Later, experiments have shown that the actual time scale of this process is about 500 fs [21]. This could stretch the time scales while keeping the picture valid. Future MD simulations would be of interest to reproduce the entire fluence dependence of structural instabilities, and including the emission of ions and charged clusters of carbon at fluences close to the damage threshold of 130 $mJ/cm^2$ [7,8].

In conclusion, the ultrafast structural dynamics of graphite obtained by means of time-resolved electron crystallography reveal the nature of atomic motions under the influence of the quasi-2D lattice potential. Following the impulsive laser excitation, the crystal undergoes a contraction followed by a strong expansion along the $c$ axis, indicating the influence of electronic band anisotropy and structural instability by coherent phonon generation. The coherent motion is evident in the diffraction, and it is the collective carrier and phonon dynamics in the first picosecond which determine the extent of layers collisions and ultimately to graphene sheet ablation (see Fig. 4). The experimental observations are consistent with theoretical simulations of ablation. Although the collision model is still valid, the time scales used in the theory require further investigations.

This work was supported by the National Science Foundation and by the Gordon and Betty Moore center for physical biology at Caltech. F. Carbone would like to thank the Swiss National Science Foundation, and also A. B. Kuzmenko for stimulating discussions. The authors thank Professor Marlina A. Elburg and Dr. S. L. Molodtsov for providing the raw crystals.

[1] M. M. J. Treacy, T. W. Ebbesen, and J. M. Gibson, Nature (London) **381**, 678 (1996).
[2] P. G. Collins *et al.*, Science **278**, 100 (1997).
[3] A. Javey *et al.*, Phys. Rev. Lett. **92**, 106804 (2004).
[4] R. H. Telling, C. P. Ewels, A. A. El-Barbary, and M. I. Heggie, Nat. Mater. **2**, 333 (2003).
[5] J. M. Zazula and S. Peraire, LHC Project Report, also Workshop on Simulating Accelerator Radiation Environment (SARE-3) May 1997 at KeK, (Tsukuba, Japan).
[6] M. S. Dresselhaus, *Graphite Fibers and Filaments* (Springer, Berlin, 1988).
[7] M. Lenner, A. Kaplan, and R. E. Palmer, Appl. Phys. Lett. **90**, 153119 (2007).
[8] A. Kaplan, M. Lenner, and R. E. Palmer, Phys. Rev. B **76**, 073401 (2007).
[9] H. O. Jeschke, M. E. Garcia, and K. H. Bennemann, Phys. Rev. Lett. **87**, 015003 (2001).
[10] K. Seibert *et al.*, Phys. Rev. B **42**, 2842 (1990).
[11] D. H. Reitze, X. Wang, H. Ahn, and M. C. Downer, Phys. Rev. B **40**, 11 986 (1989).
[12] T. Mishina, K. Nitta, and Y. Masumoto, Phys. Rev. B **62**, 2908 (2000).
[13] P. Baum, and A. H. Zewail, Proc. Natl. Acad. Sci. U.S.A. **103**, 16 105 (2006).
[14] P. Trucano and R. Chen, Nature (London) **258**, 136 (1975).
[15] A. Gruneis *et al.*, arXiv:0704.2682 [Phys. Rev. Lett. (to be published)].
[16] C-Y. Ruan, Y. Murooka, R. K. Ramani, and R. A. Murdick, Nano Lett. **7**, 1290 (2007).
[17] D. -S. Yang, N. Gedik, and A. H. Zewail, J. Phys. Chem. C **111**, 4889 (2007).
[18] T. Pfeifer, W. Kutt, H. Kurz, and R. Scholz, Phys. Rev. Lett. **69**, 3248 (1992).
[19] H. D. Fuchs, C. H. Grein, R. I. Devlen, J. Kuhl, and M. Cardona, Phys. Rev. B **44**, 8633 (1991).
[20] T. Kampfrath, L. Perfetti, F. Schapper, C. Frischkorn, and M. Wolf, Phys. Rev. Lett. **95**, 187403 (2005).
[21] G. Moos, C. Gahl, R. Fasel, M. Wolf, and T. Hertel, Phys. Rev. Lett. **87**, 267402 (2001).
[22] J. Maultzsch, S. Reich, C. Thomsen, H. Requardt, and P. Ordejon, Phys. Rev. Lett. **92**, 075501 (2004).
[23] N. Mounet and N. Marzari, Phys. Rev. B **71**, 205214 (2005).
[24] S. Piscanec, M. Lazzeri, F. Mauri, A. C. Ferrari, and J. Robertson, Phys. Rev. Lett. **93**, 185503 (2004).
[25] R. Nicklow, N. Wakabayashi, and H. G. Smith, Phys. Rev. B **5**, 4951 (1972).